INTERNATIONAL JOURNAL FOR NUMERICAL METHODS IN FLUIDS, VOL. 24, 441–455 (1997)

MIXED TRANSFORM FINITE ELEMENT METHOD FOR SOLVING THE NON-LINEAR EQUATION FOR FLOW IN VARIABLY SATURATED POROUS MEDIA

R. G. BACA

Center for Nuclear Waste Regulatory Analyses, Southwest Research Institute, San Antonio, TX 78238-5166, U.S.A.

J. N. CHUNG

Washington State University, Pullman, WA, U.S.A.

AND

D. J. MULLA

University of Minnesota, St. Paul, MN, U.S.A.

SUMMARY

A new computational method is developed for numerical solution of the Richards equation for flow in variably saturated porous media. The new method, referred to as the mixed transform finite element method, employs the mixed formulation of the Richards equation but expressed in terms of a partitioned transform. An iterative finite element algorithm is derived using a Newton–Galerkin weak statement. Specific advantages of the new method are demonstrated with applications to a set of one-dimensional test problems. Comparisons with the modified Picard method show that the new method produces more robust solutions for a broad range of soil–moisture regimes, including flow in desiccated soils, in heterogeneous media and in layered soils with formation of perched water zones. In addition, the mixed transform finite element method is shown to converge faster than the modified Picard method in a number of cases and to accurately represent pressure head and moisture content profiles with very steep fronts.

KEY WORDS: finite elements; Richards equation; porous flow

1. INTRODUCTION

The physics of isothermal flow in variably saturated porous media is largely captured in the mathematical model referred to as the Richards equation.[1] The descriptive capability of this model has popularized it as the 'knowledge engine' for many one-dimensional (1D) computer models,[2,3] as well as for sophisticated three-dimensional computer codes describing flow in highly heterogeneous porous media.[4,5] The generation of physical insights through high-resolution numerical simulations, however, has been limited because of the difficulty in obtaining rapidly convergent and accurate numerical solutions for realistic problems. This is particularly the circumstance for simulation problems involving wetting fronts moving into a desiccated soil, unsaturated flow in layered soils with sharp contrasts in hydraulic properties, as well as the formation and dissipation of perched water zones.

CCC 0271–2091/97/050441–15

Received 21 April 1995
Revised 17 June 1996

Two primary sources of numerical difficulty are (i) the strongly non-linear nature of the Richards equation and (ii) its unique mathematical character, which can change from parabolic, to hyperbolic or to elliptic behaviour. The standard prescription for accommodating the non-linearity has been to utilize an iterative method such as Newton–Raphson or Picard algorithm[6] in conjunction with finite difference or finite element approximations.[7] The ability of the Richards equation to simultaneously exhibit behaviour of the three archetypal partial differential equations in the same simulation is particularly daunting. This mathematical character is a function of the flow regime and soil hydraulic properties. For earth materials with certain soil–moisture retention properties, capillarity will dominate moisture transport and, as a result, the governing equation is a non-linear parabolic equation. In more drainable materials and at relatively high saturation levels, gravity generally dominates and induces the propagation of a steep wetting front which is characteristic of a hyperbolic equation. In the case of fully saturated conditions the governing flow equation simplifies to a linear elliptic equation. The 'multiple personalities' of the Richards equation pose a special difficulty for a computational algorithm, because it must be capable of accommodating all three types of partial differential equations.

A mixed transform finite element method is developed and applied to a set of challenging flow problems in variably saturated porous media. The capability of this new numerical method is demonstrated through direct comparisons with solutions produced with the widely popular modified Picard method.[8]

2. GOVERNING FLOW EQUATION

The partial differential equation (PDE) for flow in a variably saturated porous medium was originally derived by Richards by combining the mass conservation equation with the Buckingham–Darcy flux law. The Richards equation provides an average macroscopic description of fluid flow processes that are essentially probabilistic in nature and occur at the microscopic level. In 1D the PDE is written as

$$\frac{\partial \theta}{\partial t} = \frac{\partial}{\partial z}\left[K(h)\left(\frac{\partial h}{\partial z} - 1\right)\right], \tag{1}$$

where $\theta(h)$ is the volumetric water content (cm^3/cm^3), $K(h)$ is the hydraulic conductivity (cm s^{-1}), z is the depth (cm) taken positive downwards and h is the pressure head in centimetres of water. This PDE is commonly referred to as the mixed formulation of the Richards equation. Storage associated with compressibility of the porous medium and fluid is neglected, although it can be easily and very effectively incorporated into equation (1), e.g. using the approach of Paniconi *et al.*[9]

Two alternative forms of this PDE are the so-called h- and θ-based PDEs.[1] The standard h-based formulation, which is the more popular of the two, is expressed as

$$C(h)\frac{\partial h}{\partial t} = \frac{\partial}{\partial z}\left[K(h)\left(\frac{\partial h}{\partial z} - 1\right)\right], \tag{2}$$

with the moisture capacity term defined as $C(h) = \partial\theta/\partial h$. The θ-based formulation is

$$\frac{\partial \theta}{\partial t} = \frac{\partial}{\partial z}\left(D(\theta)\frac{\partial \theta}{\partial z} - K\right), \tag{3}$$

with the moisture diffusivity defined as $D(\theta) = K(\theta)/C(\theta)$. The classical h-based formulation has the advantages of being applicable to both saturated and unsaturated conditions and of accommodating heterogeneous soils. However, numerical approximations of this formulation generally exhibit very poor preservation of global mass balance[8,10] and relatively slow convergence. In contrast, the

classical θ-based formulation is limited to strictly unsaturated conditions and homogeneous media (i.e. θ is discontinuous at the layer interfaces). When approximated, however, it produces very well-behaved, mass-conservative and rapidly convergent solutions.[11]

Celia *et al.*[8] developed a semidiscrete 'delta' formulation of equation (1) which is referred to as the modified Picard method. This method apparently combines the benefits of both h- and θ-based PDEs without the inherent drawbacks of each formulation. Of particular importance is the mass-conservative nature of this delta formulation. This formulation is expressed as

$$C(h^k)\frac{\delta}{\Delta t} = \frac{\partial}{\partial z}\left[K(h^k)\left(\frac{\partial \delta}{\partial z} - 1\right)\right] + \frac{\partial}{\partial z}\left(K(h^k)\frac{\partial h^k}{\partial z}\right) - \frac{\Delta \theta^k}{\Delta t}, \tag{4}$$

where $\delta = h^{n+1,k+1} - h^{n+1,k}$, $\Delta\theta^k = \theta^{n+1,k} - \theta^n$ and n and k are the time plane and iteration indices respectively.

Similarly, Hills *et al.*[12] and Kirkland *et al.*[13] harvested the advantages of both the h- and θ-based formulations by introducing a generalized variable Φ which is a linear transform of pressure head and moisture content. They derive a modified form of the Richards equation, namely

$$F\frac{\partial \Phi}{\partial t} = \frac{\partial}{\partial z}\left(\frac{K}{G}\frac{\partial \Phi}{\partial z} - K\right) - \frac{\partial}{\partial z}\left(\frac{K}{G}\frac{\partial g}{\partial z}\right), \tag{5}$$

where $\Phi = \Phi(z, t) = g[h(z, t), z]$, $\theta = \theta(z, t) = f[h(z, t), z]$, $F = (\partial f/\partial h)\partial h/\partial \Phi$ and $G = \partial g/\partial h$. The last term in (5) accounts for the 'jump conditions' in the soil properties at layer interfaces. Two very significant advantages of this unique formulation are that the numerical algorithm does not require iteration and is mass-conservative. However, because (5) requires that Φ be uniquely defined, it can only be solved using a finite volume analogue with cell-centred nodes, so that discontinuous changes occur at the cell interface. Other disadvantages of this approach are associated with the calculation of G and $\Delta\Phi$ at the layer interfaces.[13]

It will be subsequently demonstrated that the modified PDE expressed in (5) is unnecessary and a finite element analogue can indeed by used with node points located at the material interfaces. In addition, the computational advantages of the new mixed transform method are illustrated through comparisons against the modified Picard method.

3. MIXED TRANSFORM FORMULATION

Using a transform similar to that of Kirkland *et al.*,[13] a mixed formulation of the Richards equation can be developed in terms of the partitioned transformed variable χ:

$$\frac{\partial \theta}{\partial t} = \frac{\partial}{\partial z}\left(K\frac{\partial h}{\partial \chi}\frac{\partial \chi}{\partial z} - K\right), \tag{6}$$

where

$$\chi = \begin{cases} h, & h \geqslant h_0, \\ \alpha_1\theta + \alpha_2, & h < h_0, \end{cases} \tag{7}$$

with the transform coefficients

$$\frac{\partial h}{\partial \chi} = \begin{cases} 1, & h \geqslant h_0, \\ 1/\alpha_1 C(h), & h < h_0, \end{cases} \tag{8}$$

$$\alpha_1 = 1/C(h_0), \tag{9}$$

$$\alpha_2 = h_0 - \alpha_1\theta_0. \tag{10}$$

The transition pressure head h_0 is an arbitrary parameter, with θ_0 being the corresponding water content value. It is easy to verify that for $h \geqslant h_0$, direct substitution of (7) and (8) into (6) yields the h-based form. Similarly, for $h < h_0$, equation (6) transforms to the θ-based form. From equation (7) it is evident that the benefits of the partitioned transform can be maximized by choosing a transition pressure value close to zero. This choice has the effect of making the transformed PDE behave (numerically) much more like the classical θ-based formulation expressed in equation (3). Through numerical experiments, Kirkland *et al.*[13] empirically selected a value of -15 cm. In this study, however, it was found that an h_0-value close to the air entry pressure h_a yielded the most consistent results.

4. FINITE ELEMENT ALGORITHM

An iterative algorithm is formulated using the elegantly simple Galerkin finite element procedure, which requires that the integral over the domain of the residual ε and a set of weighting functions ω_j vanishes. Thus the Galerkin functional is

$$\Omega_G = \int_0^L \omega_j \varepsilon \mathrm{d}z = 0 \quad (j = 1, 2, \ldots, N), \tag{11}$$

where the residual is obtained directly from (6), namely

$$\varepsilon = \frac{\partial \theta}{\partial t} - \frac{\partial}{\partial z}\left(K \frac{\partial h}{\partial \chi}\frac{\partial \chi}{\partial z} - K \right). \tag{12}$$

In this expression the quantities θ, χ and K are approximated in terms of a set of linear basis functions; these functions are chosen to be identical to the set of weighting functions ω_j. Since the residual is non-linear, it is useful to expand ε in terms of a Taylor series.[14] Thus the Newton–Galerkin functional is

$$\Omega_{NG} = \int_0^L \omega_j \left(\varepsilon^k + \frac{\partial \varepsilon^k}{\partial h}\Delta h \right) \mathrm{d}z = 0 \quad (j = 1, 2, \ldots, N), \tag{13}$$

where k is the iteration index. It is important to note that the Taylor series is expanded in terms of h rather than θ or χ, which are discontinuous. Choosing h as the solution variable has the advantage cited previously for the h-based formulation. The nodal values of pressure head h_j at the new time plane $n+1$ and the new iterate $k+1$ are computed using the Newton iteration formula

$$h_j^{k+1} = h_j^k + \Delta h_j^k. \tag{14}$$

Rearranging the quantities in (13) and expressing them in matrix notation produces

$$[J]\{\Delta h\} = -\{R\}, \tag{15}$$

where the right-hand-side vector $\{R\}$ and the Jacobian matrix $[J]$ are

$$\{R\} = \int_0^L \omega_j \varepsilon^{(k)} \mathrm{d}z, \qquad [J] = \int_0^L \omega_j \frac{\partial \varepsilon^{(k)}}{\partial h} \mathrm{d}z. \tag{16}$$

Discretizing $\partial\theta/\partial t$ and integrating by parts, the components of the Newton–Galerkin 'weak statement' become

$$\{R\} = \frac{1}{\Delta t}\int_0^L \omega_j(\theta^{n+1,k} - \theta^n)\mathrm{d}z + \int_0^L \frac{\partial\omega_j}{\partial z}\left(\kappa\frac{\partial\chi}{\partial z} - K\right)^{n+1,k}\mathrm{d}z - \omega_j\left(\kappa\frac{\partial\chi}{\partial z} - K\right)_0^L, \tag{17}$$

$$[J] = \frac{1}{\Delta t}\int_0^L \omega_j\left(\frac{\partial\theta}{\partial h}\right)^{n+1,k}\mathrm{d}z + \int_0^L \frac{\partial\omega_j}{\partial z}\left[\kappa\frac{\partial}{\partial h}\left(\frac{\partial\chi}{\partial z}\right) + \frac{\partial\kappa}{\partial h}\frac{\partial\chi}{\partial z} - \frac{\partial K}{\partial h}\right]^{n+1,k}\mathrm{d}z, \tag{18}$$

where $\kappa = K\partial h/\partial\chi$ and $\partial\kappa/\partial h \approx (\partial K/\partial h)\partial h/\partial\chi$. In the latter approximation the term $K\partial h^2/\partial\chi^2$ was neglected because it was found to be small. The integration by parts in the previous equations effectively reduced or 'weakened' the differentiation requirement[15] on χ. Inserting the expressions for the linear basis functions $\omega_1 = 1 - \xi/L_\mathrm{e}$ and $\omega_2 = \xi/L_\mathrm{e}$, the individual terms of (17) and (18) can be integrated exactly using[15]

$$\int_0^1 \xi_1^a\xi_2^b\mathrm{d}l = L_\mathrm{e}\frac{a!b!}{(a+b+1)!}, \tag{19}$$

where ξ is the local element co-ordinate, (a, b) are integers and L_e is the element length. For a generic finite element of length L_e the elemental matrices are

$$\{R_\mathrm{e}\} = \frac{1}{\Delta t}\left(\frac{L_\mathrm{e}}{2}\right)\{\Delta\theta^k\} - \bar{K}\begin{Bmatrix}-1\\1\end{Bmatrix} + \frac{1}{L_\mathrm{e}}\bar{\kappa}\Delta\chi^k\begin{Bmatrix}-1\\1\end{Bmatrix} - \begin{Bmatrix}q_0^{\mathrm{bc}}\\-q_l^{\mathrm{bc}}\end{Bmatrix}, \tag{20}$$

$$\begin{aligned}[J_\mathrm{e}] = {} & \frac{1}{\Delta t}\left(\frac{L_\mathrm{e}}{2}\right)\begin{bmatrix}\partial\theta_1/\partial h_1 & 0\\ 0 & \partial\theta_2/\partial h_2\end{bmatrix}\\ & + \frac{1}{L_\mathrm{e}}\bar{\kappa}\begin{bmatrix}\partial\chi_1/\partial h_1 & -\partial\chi_2/\partial h_2\\ -\partial\chi_1/\partial h_1 & \partial\chi_2/\partial h_2\end{bmatrix}\\ & + \frac{\Delta\chi^k}{L_\mathrm{e}}\begin{bmatrix}-\partial\bar{\kappa}/\partial h_1 & -\partial\bar{\kappa}/\partial h_2\\ \partial\bar{\kappa}/\partial h_1 & \partial\bar{\kappa}/\partial h_2\end{bmatrix}\\ & - \begin{bmatrix}-\partial\bar{K}/\partial h_1 & -\partial\bar{K}/\partial h_2\\ \partial\bar{K}/\partial h_1 & \partial\bar{K}/\partial h_2\end{bmatrix},\end{aligned} \tag{21}$$

with $\Delta\theta^k = \theta^{n+1,k} - \theta^n$ and $\Delta\chi^k = (\chi_2 - \chi_1)^{n+1,k}$; $\bar{\kappa}$ and $\bar{K}$ are the average values (e.g. arithmetic, geometric or harmonic) for the element. If prescribed, the flux terms q_0^{bc} and q_L^{bc} contribute to $\{R\}$ at the top and bottom boundaries; in the interior of the domain they are of course self-cancelling. Mass lumping has been used in (20) and (21) to stabilize the matrices associated with the θ-terms.

In implementing the new finite element algorithm, termination of the Newton iteration process is based on a dual convergence criterion which tests the norms of relative change and residual vectors. Specifically, the numerical solution must satisfy

$$\max|\Delta h_j/h_j| \leqslant \varepsilon_{\mathrm{rel}} \quad \text{and} \quad \| r^{(k+1)} \|_\infty \leqslant \varepsilon_{\mathrm{res}}, \tag{22}$$

where $\| \ \|_\infty$ is the infinity norm and $r^{(k+1)}$ is the residual computed as $J\Delta h^{(k+1)} + R$.

In general the maximum relative change is a good indicator of convergence; however, the residual norm is more stringent and reliable. Typical ranges of values for the control tolerances in equation (22) are $10^{-6} \leqslant \varepsilon_{\mathrm{rel}} \leqslant 10^{-3}$ and $10^{-8} \leqslant \varepsilon_{\mathrm{res}} \leqslant 10^{-5}$.

5. COMPUTATIONAL TEST PROBLEMS

A 1D computer code was written in FORTRAN 77 to implement the mixed transform finite element algorithm. For the purpose of making comparisons, a second finite element computer code was developed using the modified Picard method. The two codes were verified through intercomparisons with the UNSAT1D code[2] and BREATH code.[3] Both codes developed for this study included options for numerical solutions using uniform time steps, over specified time intervals, and fully automatic time stepping. All computer runs were performed on an IBM PS/2 Model 95 (66 MHz).

Three challenging computational test problems, taken directly from the hydrology and soil physics literature, were selected to demonstrate the capabilities of the mixed transform finite element approach. The nature and level of computational difficulties associated with the selected test problems were characterized in terms of the grid hydraulic Peclet number Pe_{hg} and hydraulic time scale parameter τ_{hg}. As in heat and mass transfer, the hydraulic Peclet number describes the relative significance of convective to diffusive transport. A Peclet number $Pe_{hg} > 2$ means that the gravity term in the Richards equation is becoming dominant and implies that a fine grid may be necessary to capture a sharp pressure front. The grid hydraulic Peclet number[16,17] is calculated from

$$Pe_{hg} = -\frac{\partial}{\partial h}[\ln K(h)]\Delta z, \tag{23}$$

where Δz is the element size. For gravity-driven flow the time scale parameter can be estimated using a hydraulic Courant number (by analogy to its use in computational fluid dynamics) Co_{hg} from the relation

$$\tau_{hg} = \frac{Co_{hg}}{Pe_{hg}}\frac{\Delta z}{K(h)}. \tag{24}$$

For fully implicit algorithms such as that used here, Co_{hg} can be chosen to be greater than unity. For diffusion- or capillarity-dominated moisture transport the hydraulic time scale parameter can be estimated using a relation similar to that for the time constant of heat conduction,[18] namely

$$\tau_{hg} = \frac{\Delta z^2}{K(h)/C(h)}. \tag{25}$$

Zones close to fully saturated conditions generally exhibit smaller characteristic times and thus control the time stepping for the entire domain. Typically, the maximum time step size should be comparable with the minimum τ_{hg} in order to capture the transient changes in pressure head occurring across an element.

5.1. Test Problem 1—Flow into a desiccated soil column

The first computational problem is adapted from a flow simulation previously used by Celia *et al.*[8] to test numerical techniques for solving the Richards equation. This test problem involves modelling a wetting front moving through a homogeneous, vertical soil column. This deceptively simple flow problem is fairly challenging because of the imposed Dirichlet boundary conditions, strongly non-linear soil hydraulic properties and relatively large pressure head gradients. The idealized soil column is 60 cm in length and is assumed to consist of desert soil representative of the Las Cruces field site in

New Mexico. Flow in the soil column occurs as a result of the specified pressure head at the surface, gravity and capillarity effects. The bottom boundary is held at the initial pressure head h_i. The soil hydraulic properties are described by the van Genuchten[19] relations

$$S_e = \frac{\theta - \theta_r}{\theta_s - \theta_r} = \left(\frac{1}{1 + (\alpha|h|)^n}\right)^m, \tag{26}$$

$$K = K_s S_e^{1/2}[1 - (1 - S_e^{1/m})^m]^2, \tag{27}$$

where θ_r and θ_s are the residual and saturated water contents respectively, K_s is the saturated hydraulic conductivity and α, n and m are model parameters with $m = 1 - 1/n$. Values for these parameters are $\theta_r = 0{\cdot}102$, $\theta_s = 0{\cdot}368$, $K_s = 9{\cdot}22 \times 10^{-3}$ cm s^{-1}, $\alpha = 0{\cdot}0335$ cm^{-1} and $n = 2$. The air entry pressure for this case is computed from $h_a = -1/\alpha$ and the transition pressure from $h_0 = h_a - 1$.

To make the problem progressively more challenging, four cases were considered in which the top boundary pressure h_b was varied, namely $h_b = -75, -25, 0$ and 75 cm. The initial pressure head in the soil column was uniform and set to a value of $h_i = -1000$ cm. As in Reference 8, a uniform mesh of two-node line elements was used to represent the vertical soil column with $\Delta z = 2{\cdot}5$ cm. The mixed transform simulations were performed using automatic time stepping with 'starting' step sizes of $0{\cdot}1 \leqslant \Delta t \leqslant 20$ s, depending on the case. Convergence of the iteration algorithm was defined by the tolerances $\varepsilon_{rel} \leqslant 10^{-4}$ and $\varepsilon_{res} \leqslant 10^{-6}$.

Comparisons of the pressure head profiles obtained with the mixed transform and modified Picard methods are shown in Figure 1. For the coarse mesh used, the graphical comparisons of numerical results show satisfactory agreement except in the location of the front. To resolve this difference, the simulation with the mixed transform code was reported with a finer mesh (i.e. $\Delta z = 1$ cm) and smaller time steps. The fine grid solution, also presented in Figure 1, shows closer agreement with the original mixed transform solutions.

Iteration histories for the cases of 'wet' boundary condition ($h_b = 0$ cm) and 'dry' boundary condition ($h_b = -75$ cm) were generated for solutions obtained with uniform time steps within time intervals. These iteration histories are compared in Figure 2. These histories clearly show that the mixed transform method exhibits much faster convergence, particularly for the wet boundary condition case. It is also clear that the modified Picard method, while quite robust and competitive for

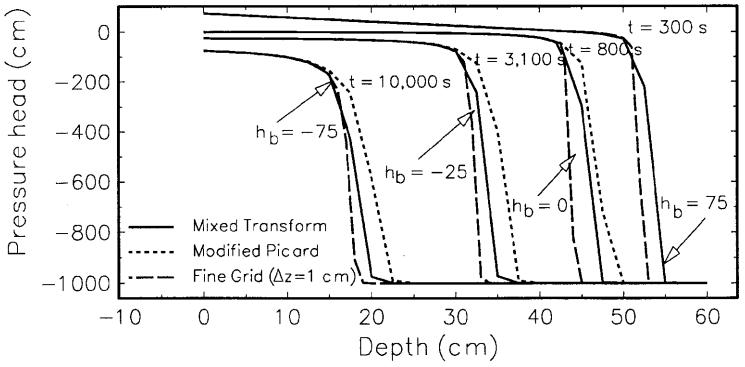

Figure 1. Comparison of mixed transform and modified Picard solutions for Test Problem 1: $h_b = -75$, -25, 0 and 75 cm; soil column discretized using uniform grid, $\Delta z = 2{\cdot}5$ cm

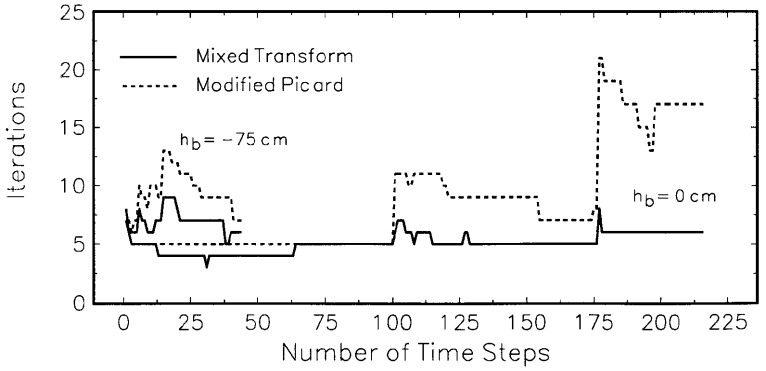

Figure 2. Iteration histories for mixed transform (full line) and modified Picard (broken line) solutions for bounding cases of Test Problem 1

dry initial conditions, exhibits a strong sensitivity to wet and ponded boundary conditions. This numerical characteristic of the modified Picard method has not been highlighted in the existing literature.[8,20]

The numerical characteristics suggested by the iteration histories are supported by the central processing unit (CPU) times for the four cases. The CPU times, which are listed in Table I, show that the mixed transform is generally faster than the modified Picard method. For the wet case the mixed transform method was about 2·5–6·5 times faster than the modified Picard solution. In addition, it was found that for the case with the 'ponded' boundary condition ($h_b = 75$ cm) the modified Picard solution required very small time steps and high iteration limits (i.e. 100 iterations) to produce a convergent solution.

Insight into the numerical characteristics of this test problem can be gleaned from the Pe_{hg} and τ_{hg} curves shown in Figure 3. For the two unsaturated boundary conditions the Pe_{hg} curves show a front-like shape with the maximum value occurring at the top boundary. The wet or saturated boundary conditions case, however, exhibits a maximum Pe_{hg}-value near the location of the wetting front. In the case of the ponded boundary condition the curve is completely distinct and almost completely flat with $Pe_{hg} \ll 1$. The sequence of τ_{hg} curves, however, shows more consistent trends. These hydraulic response times are small in magnitude and relatively uniform behind the wetting front and then rapidly transit to very large values. The small τ_{hg}-values behind the wetting front constrain the magnitude of allowable time steps.

5.2. Test Problem 2—Flow into a dry layered soil

The second test problem, originally solved by Hills *et al.*,[12] involves modelling infiltration into a field-scale layered lysimeter. This test problem is an excellent one because it poses a strongly non-linear flow problem that exhibits very large gradients in both pressure head and moisture content. Five soil layers (each 20 cm) consisting of alternating Bernino loamy fine sand and Glendale clay

Table I. Comparison of CPU times for Test Problem 1

	CPU time (s)			
Method	$h_b = -75$	$h_b = -25$	$h_b = 0$	$h_b = 75$
Mixed Transform	4	7	12	14
Modified Picard	11	16	35	92

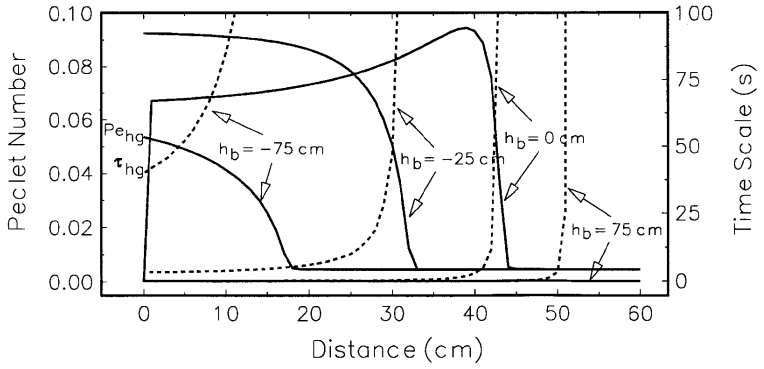

Figure 3. Hydraulic Peclet number (full line) and time scale (broken line) curves for Test problem 1: results for fine grid solutions ($\Delta z = 1$ cm)

loam make up the 100 cm soil column. The soil hydraulic properties are described by the van Genuchten[19] formulae. For the Bernino loamy fine sand these parameters are $\theta_r = 0{\cdot}0286$, $\theta_s = 0{\cdot}3658$, $K_s = 541{\cdot}0$ cm day^{-1}, $\alpha = 0{\cdot}0280$ cm^{-1} and $n = 2{\cdot}2390$. For the Glendale clay loam the soil hydraulic parameters are $\theta_r = 0{\cdot}1060$, $\theta_s = 0{\cdot}4686$, $K_s = 13{\cdot}1$ cm day^{-1}, $\alpha = 0{\cdot}0104$ cm^{-1} and $n = 1{\cdot}3954$. The air entry pressure for this case was computed from $h_a = -1/\alpha$ and the transition pressure from $h_0 = \max(h_a)_j - 1$, where j is the soil material index.

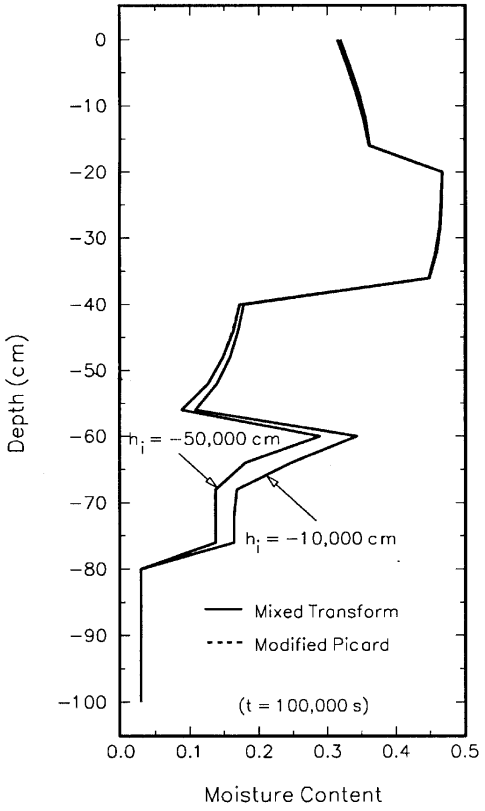

Figure 4. Moisture content profiles computed for Test Problem 2 using mixed tranform and modified Picard methods; soil column discretized using uniform grid, $\Delta z = 4$ cm

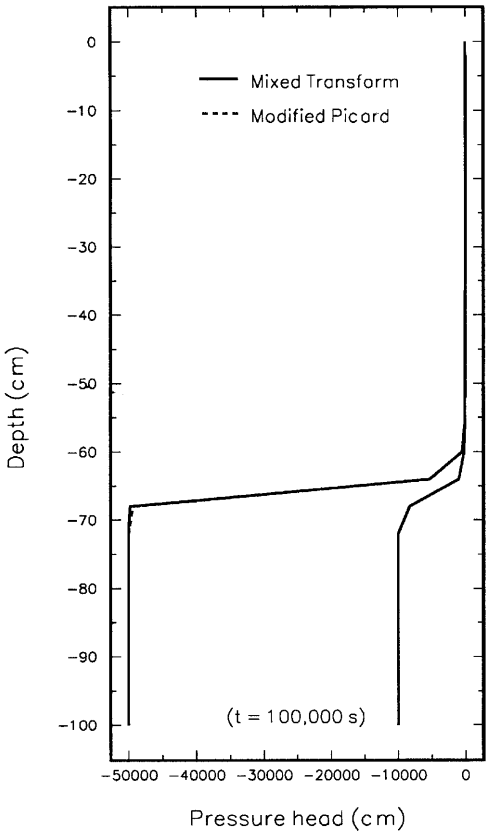

Figure 5. Comparison of pressure head profiles computed for Test Problem 2; soil column discretized using uniformm grid, $\Delta z = 4$ cm

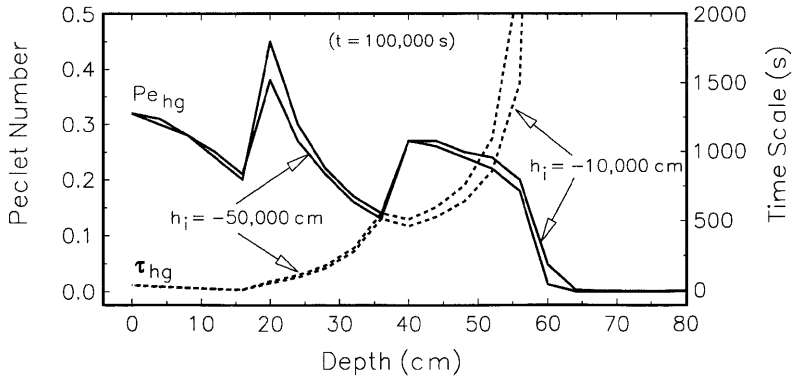

Figure 6. Hydraulic Peclet number (full line) and time scale (broken line) curves for Test Problem 2

Two cases of increasing computational difficulty were simulated in which the initial pressure head profile was set to $h_i = -10^4$ and -5×10^4 cm. The upper boundary condition was a constant flux of $q_0^{bc} = 13{\cdot}1$ cm day^{-1} at the soil surface, which is exactly equal to the hydraulic conductivity of the clay loam layer. The bottom boundary was held at the initial pressure head. The flow domain was discretized into a uniform mesh of finite elements with $\Delta z = 4$ cm. A time domain of 10^5 s was simulated using automatic time stepping steps of 5·0 and 0·2 s for the dry and drier initial conditions respectively. The convergence tolerances were set to $\varepsilon_{rel} \leqslant 10^{-4}$ and $\varepsilon_{res} \leqslant 10^{-6}$.

The moisture content profiles computed at the end of the simulation period are shown in Figure 4; because the moisture content is discontinuous at material interfaces, the nodal values at these interfaces were calculated using the hydraulic properties of the lower soil. In this figure the numerical results obtained for both initial conditions are compared. The results produced by the mixed transform finite element method agree exceptionally well with those computed with the modified Picard method. As illustrated in Figure 5, the two computed pressure head profiles overlay nearly perfectly.

Although both cases exhibit very large pressure gradients, quite interestingly, neither case was especially taxing for either the mixed transform or the modified Picard method. The CPU times for the first case ($h_i = -10^4$ cm) were 13 s for the mixed transform solution and 20 s for the modified Picard solution, indicating that the mixed transform is almost twice as fast. For the second case ($h_i = -5 \times 10^4$ cm) the mixed transform method required 17 s and the modified Picard method required 22 s. This comparison of CPU times clearly shows that both methods exist low sensitivity to very dry initial conditions.

The Pe_{hg} and τ_{hg} curves for the two cases are quite similar to each other, as illustrated in Figure 6. It is noted that the Peclet number and time scale parameter values for this test problem are more constraining at the end of the simulation than at the beginning. The curves are illustrated in Figure 6; they suggest that the first two layers are largely capillary-dominated and exhibit the smaller hydraulic response times.

5.3. Test Problem 3—Variably saturated flow into a layered soil

The final test problem is taken from Reference 21 and involves flow into a layered soil column. A high-flux boundary condition, relative to the soil hydraulic conductivity, creates locally saturated and unsaturated regions. The physical setting consists of a thin surface crust (0·5 cm), a tilled layer (10 cm) and an undisturbed subsoil layer (15 cm). At the surface the water application rate is $q_0^{bc} = 10$ cm h^{-1}, while the bottom boundary is held at a fixed pressure head value equal to the initial value. The soil hydraulic properties for each layer are described by the Brooks–Corey formulae[21]

$$\theta(h) = \begin{cases} \theta_s, & h \geqslant h_a, \\ \theta_s (h/h_a)^{-1/b}, & h < h_a, \end{cases} \tag{28}$$

$$K(h) = \begin{cases} K_s, & h \geqslant h_a, \\ K_s (h/h_a)^{-n}, & h < h_a, \end{cases} \tag{29}$$

where h_a is the air entry value of the pressure head and b and n are fitting parameters with $n = 2 + 3/b$. The parameter values for (i) the surface crust are $\theta_s = 0{\cdot}562$, $K_s = 0{\cdot}0616$ cm h^{-1}, $h_a = -4{\cdot}55$ cm and $b = 6{\cdot}8$, (ii) the tilled layer are $\theta_s = 0{\cdot}562$, $K_s = 1{\cdot}396$ cm h^{-1}, $h_a = -4{\cdot}55$ cm

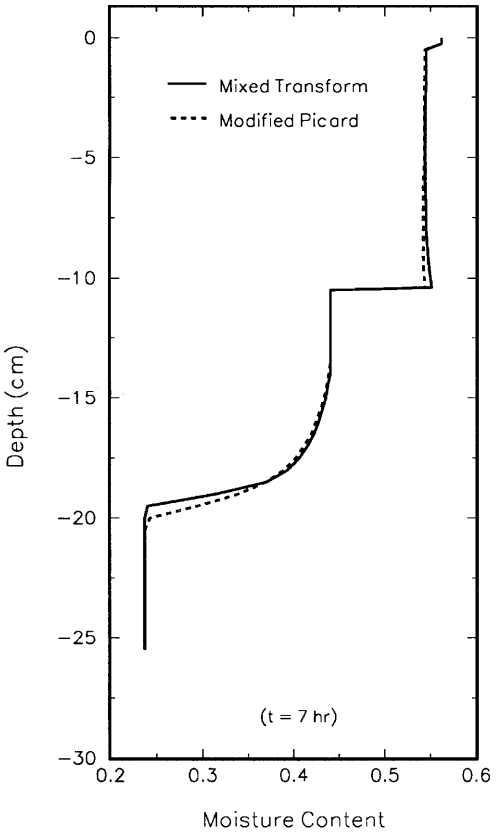

Figure 7. Comparison of moisture content profiles computed for Test Problem 3 using mixed transform and modified Picard methods

and $b = 13{\cdot}3$ and (iii) the undisturbed subsoil $\theta_s = 0{\cdot}440$, $K_s = 0{\cdot}312$ cm h^{-1}, $h_a = -9{\cdot}50$ and $b = 13{\cdot}3$. Because of the discontinuous nature of the Brooks–Corey conductivity function, a transition pressure for each soil layer was computed from $h_0 = h_a - \varepsilon$, where ε was an arbitrary small number (e.g. 10^{-3}).

The vertical soil column was represented by a variably spaced finite element mesh consisting of $\Delta z = 0{\cdot}25$ cm in the surface crust, $\Delta z = 0{\cdot}5$ cm in the tilled layer and $\Delta z = 0{\cdot}5$–$1{\cdot}0$ cm in the undisturbed subsoil layer. The initial pressure head was uniform and set to $h_i = -35{,}100$ cm. The simulation period of 7 h was simulated using automatic time stepping with a starting step of $\Delta t = 5$ s. Convergence of the mixed transform iteration algorithm was defined by the tolerances $\varepsilon_{rel} \leqslant 10^{-5}$ and $\varepsilon_{res} \leqslant 10^{-6}$.

The computed moisture content profiles for $t = 7{\cdot}0$ h are illustrated in Figure 7; the nodal values at these material interfaces were calculated using the hydraulic properties of the lower soil. In this figure the numerical solutions produced by the mixed transform finite element method are compared with those calculated with the modified Picard finite element code. The differences between the two moisture profiles are very small. The calculated pressure heat profiles, which are presented in Figure 8, also show excellent agreement. The iteration histories, which are presented in Figure 9, provide insight into the computational efficiency of the two solution techniques. From this plot it can be noted that the modified Picard method exhibits a much greater sensitivity to the time step size for this case. In fact, for the large time step size the Picard iteration process shows a large increase in iterations.

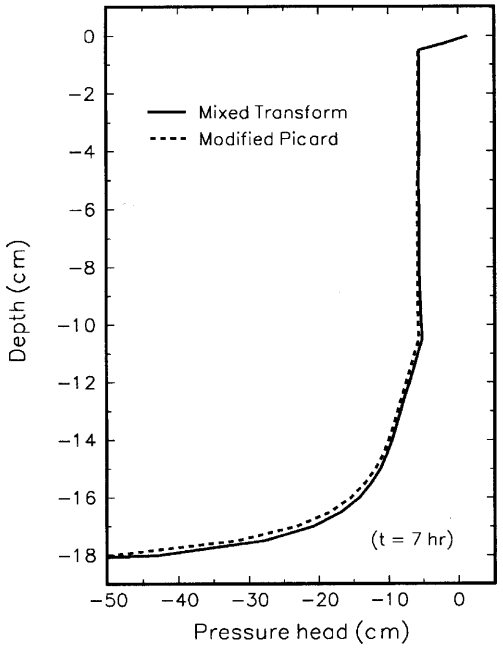

Figure 8. Comparison of pressure head profiles computed for Test Problem 3 using mixed transform and modified Picard methods

This behaviour is consistent with the iteration history observed in the first test problem. The comparison of CPU times showed that the mixed transform solution was faster than the modified Picard solution by a factor of 1·6.

The Pe_{hg} and τ_{hg} curves calculated for this test problem, shown in Figure 10, indicate that this problem was primarily dominated by capillary flow ($Pe_{hg} < 1$) and the hydraulic response times in the second layer are relatively large considering that it is almost completely saturated. These numerical characteristics explain to some degree the observation of Ross and Bristow[21] that accurate solutions for this test problem can be obtained with a coarse grid and large time steps.

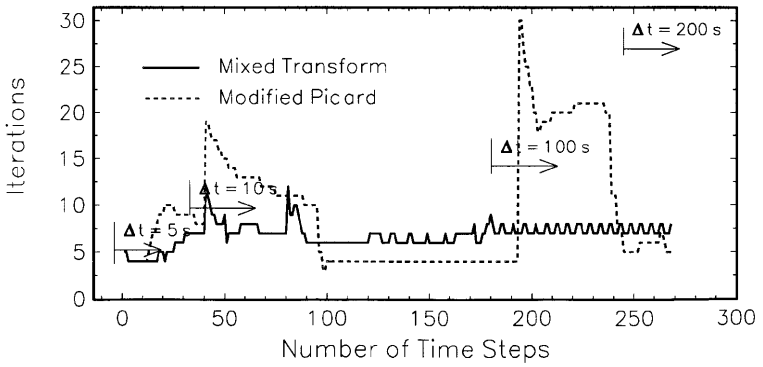

Figure 9. Iteration histories computed for Test Problem 3 using mixed transform and modified Picard methods

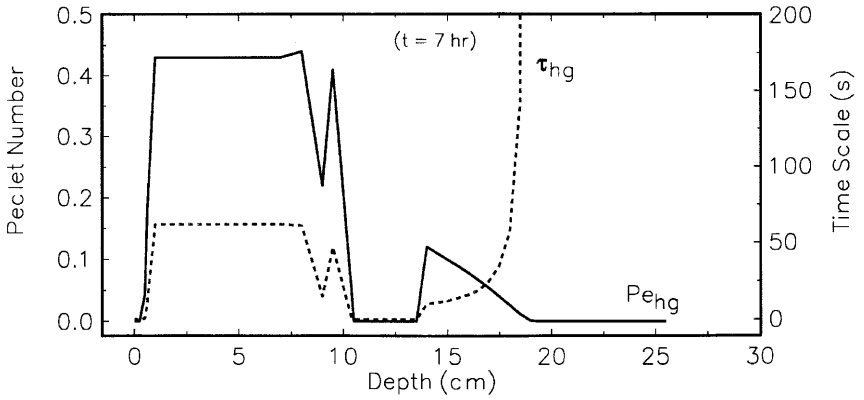

Figure 10. Hydraulic Peclet number (full line) and time scale (broken line) curves for Test Problem 3

6. CONCLUSIONS

A mixed transform finite element method was developed for solving the non-linear Richards equation for variably saturated flow. In this new approach the mixed formulation of the flow equation is transformed using a partitioned change of variable. An iterative scheme is embedded in the finite element algorithm for the transformed equation. This technique is formulated using a Newton–Galerkin weak statement. The capabilities of this new method are demonstrated with applications to a set of challenging 1D computational test problems. The hydraulic Peclet number Pe_{hg} and the characteristic time scale τ_{hg} were introduced to provide insight into the nature and level of computational difficulty of the test problems.

For the broad range of regimes considered in the test cases, the mixed transform method exhibits a higher degree of robustness than the modified Picard method. In certain cases the mixed transform method can converge faster and more accurately capture steep pressure head and moisture content profiles which are typically encountered in desiccated soils. The new method is easy to implement in existing one- and multi-dimensional finite element codes, as well as finite volume codes. The new method offers improved computational efficiency, accuracy and robustness for a broad range of variably saturated flow problems.

ACKNOWLEDGEMENTS

The authors wish to thank Drs. S. Stothoff, P. Lichtner and G. Ofoegbu of the Center for Nuclear Waste Regulatory Analyses (CNWRA) and Dr. J. Randall of the U.S. Nuclear Regulatory Commission for their review and comments on the original manuscript. The assistance of Dr. Stothoff with the application of the BREATH code is gratefully acknowledged. The research presented in this paper was funded by the Nuclear Regulatory Commission (NRC) under Contract 02-93-005 and was performed at the CNWRA. The research was performed on behalf of the NRC Office of Nuclear Regulatory Research, Division of Regulatory Applications. The paper is an independent product of the CNWRA and does not necessarily reflect the views or regulatory position of the NRC. The BREATH code used in this study is controlled under the CNWRA Software Configuration Procedure. The other codes used in the study are not yet under software configuration management.

REFERENCES

1. W. A. Jury, W. R. Gardner and W. H. Gardner, *Soil Physics*, 5th edn, Wiley, New York, 1993.
2. M. A. Celia, *The One-Dimensional Princeton Unsaturated Flow Code*, distributed at the Short Course on Fundamentals of Unsaturated Zone Modeling, Princeton, NJ, 1991.
3. S. Stothoff, *BREATH Version 1.0—Coupled Flow and Energy Transport in Porous Media, Simulator Description and User Guide, NUREG/CR-6333*, U.S. Nuclear Regulatory Commission, Washington, DC, 1995.
4. A. K. Runchal and B. Sagar, *PORFLOW—a Multifluid, Multiphase Model for Simultaneous Flow, Heat Transfer, and Mass Transport in Fractured-Porous Media, User's Manual, Version 2.41, NUREG/CR-5991*, Nuclear Regulatory Commission, Washington, DC, 1993.
5. R. Ababou and A. C. Bagtzoglou, *BIGFLOW: a Numerical Code for Simulating Flow in Variably Saturated, Heterogeneous Geologic Media, Theory and User's Manual, Version 1.1, NUREG/CR-6028*, Nuclear Regulatory Commission, Washington, DC, 1993.
6. C. Paniconi and M. Putti, 'A comparison of Picard and Newton iteration in the numerical solution of multi-dimensional variably-saturated flow problems', *Water Resources Res.*, **39**, 3357–3374 (1994).
7. P. S. Huyakorn and G. Pinder, *Computational Methods in Subsurface Flow*, Academic, New York, 1983.
8. M. A. Celia, E. T. Bouloutas and R. L. Zarba, 'A general mass-conservative numerical solution for the unsaturated flow equation', *Water Resources Res.*, **26**, 1483–1496 (1990).
9. C. Paniconi, A. A. Aldama and E. F. Wood, 'Numerical evaluation of iterative and noniterative methods for the solution of the nonlinear Richards equation', *Water Resources Res.*, **27**, 1147–1163 (1991).
10. P. C. D. Milly, 'A mass-conservative procedure for time-stepping in models of unsaturated flow', *Adv. Water Resources*, **8**, 32–36 (1985).
11. H. M. E. Selim, 'Transient and steady two-dimensional flow of water in unsaturated soils', *Ph.D. Thesis*, Iowa State University, Ames, IA, 1971.
12. R. G. Hills, I. Porro, D. B. Hudson and P. J. Wierenga, 'Modeling one-dimensional infiltration into very dry soils, 1. Model development and evaluation', *Water Resources Res.*, **25**, 1259–1269 (1989).
13. M. R. Kirkland, R. G. Hills and P. J. Wierenga, 'Algorithms for solving Richards' equation for variably saturated soils', *Water Resources Res.*, **28**, 2049–2058 (1992).
14. R. G. Baca, I. P. King and W. R. Norton, 'Finite element models for simultaneous heat and moisture transport in unsaturated soils', *Proc. Second Int. Conf. on Finite Elements in Water Resources*, Pentech, London, 1978, pp. 1.19–1.35.
15. D. W. Pepper and J. C. Heinrich, *The Finite Element Method*, Taylor and Francis, Bristol, PA, 1992.
16. B. A. Finlayson, *Nonlinear Analysis in Chemical Engineering*, McGraw-Hill, New York, 1980.
17. R. Ababou, 'Numerical analysis of nonlinear unsaturated flow equation', *Proc. Computational Methods in Subsurface Hydrology*, Springer, Berlin, 1990, pp. 151–159.
18. G. E. Meyers, *Analytical Methods in Conduction Heat Transfer*, McGraw-Hill, New York, 1971, pp. 219–222.
19. M. T. van Genuchten, 'A closed-form equaiton for predicting the hydraulic properties of unsaturated soils', *Soil Sci. Soc. Am. J.*, **44**, 892–898 (1980).
20. M. A. Celia, E. T. Bouloutas and P. Binning, 'Numerical methods for nonlinear flows in porous media', *Proc. Computational Methods in Subsurface Hydrology*, Springer, Berlin, 1990, pp. 145–150.
21. P. J. Ross and K. L. Bristow, 'Simulating water movement in layered and gradational soils using the Kirchoff transform', *Soil Sci. Soc. Am. J.*, **54**, 1519–1524 (1993).